ELSEVIER

Journal of Photochemistry and Photobiology A: Chemistry 117 (1998) 185–192

Journal of Photochemistry and Photobiology A:Chemistry

Photophysical properties of $Re(CO)_3L_3^+$ (L=monoazine) complexes Electronic delocalization effect in metal-to-ligand charge transfer excited states

M.R. Feliz[*,1], F. Rodriguez-Nieto[1], G. Ruiz[1], E. Wolcan[2]

Instituto de Investigaciones Fisicoquimicas Teoricas y Aplicadas (INIFTA), Facultad de Ciencias Exactas, Universidad Nacional de La Plata, CC16 - SUC.4, La Plata (1900), Argentina

Received 10 March 1998; received in revised form 27 May 1998; accepted 28 May 1998

Abstract

The photophysical properties of the series of the $[Re(CO)_3L_3]CF_3SO_3$ (L=4-phenylpyridine, 3-phenylpyridine, 4–benzylpyridine, 4-(4′-nitrobenzyl)-pyridine and 4,4′-bipyridine) have been studied. Emission spectral changes with temperature and biexponential decay of the luminescence both in dichloromethane fluid solution and frozen (77 K) media show two excited states, intraligand (IL) and metal-to-ligand charge transfer (MLCT) in character, emitting with intrinsic rates. Rates of MLCT emission badly correlate with the excited state-ground state energy gap. Departures from the energy gap law are rationalized in terms of excited state distortion and electronic delocalization.

Keywords: Photophysical properties; Electronic delocalization; Metal-to-ligand charge transfer (MLCT)

1. Introduction

Decay of metal-to-ligand charge transfer (MLCT) excited states of azine complexes of d^6 transition metal ions (Ru^{II}, Re^{I}, etc.) at room temperature in fluid solution are typically dominated by non-radiative processes [1–4]. Their rate constants usually increase as the energy gap between the ground and excited state decreases, consistent with the energy gap law [5–7]. As a consequence, complexes with low energy absorption bands are typically weak emitters and have short-lived excited states. Naturally, the decreased lifetimes limit their use as sensitizers in photo-induced energy and electron transfer [8–10].

The energy gap law originates in a quantum effect. The energy gap influences vibrational overlap between the initial and final states in the acceptor modes [11–13]. Simultaneously, there is a change in equilibrium displacement (Δ_M) between the initial and final electronic states, and overlap increases as Δ_M increases. The dependence of k_{nr} (rate constant for non-radiative decay) on E_{00} (energy of $\nu'=0\rightarrow\nu=0$ transition) and the excited state distortion has been experimentally verified. In this regard, ligand rigidity and electronic delocalization account for deviations from energy gap law.

We report here a study of photo-physical properties of a series of rhenium tris–monoazine complexes where deviation from the energy gap law is rationalized in terms of electronic delocalization.

2. Experimental section

2.1. Materials

The complexes $[Re(CO)_3L_3](CF_3SO_3)$ with L=3-phenylpyridine, 4,4′bipyridine, 4-benzylpyridine and 4-(4′-nitrobenzyl)-pyridine were prepared according to literature procedures [14,15]. The synthesis of the complexes involved the substitution of Cl^- from $ClRe(CO)_3L_2$ by L in the presence of $AgCF_3SO_3$. $ClRe(CO)_3L_2$ (3.2 mmol), $AgCF_3SO_3$ (3.2 mmol) and L (32 mmol) were added to 250 ml of toluene. The solution was magnetically stirred and refluxed for 9 h under a N_2 atmosphere. A large excess of the ligand was necessary to obtain an acceptable yield. The ClAg that precipitated was removed by filtration keeping the temperature between 5–10°C. The filtrate was rotoevaporated to dryness. The product, redissolved in a mini-

*Corresponding author. Fax: +54-21-254642
[1]Member of CICBA.
[2]Member of CONICET.

1010-6030/98/$ – see front matter
PII: S1010-6030(98)00323-2

mum volume of dichloromethane, was applied to a neutral alumina column for chromatography. Elution was initiated with dichloromethane until the excess of L had been removed. Elution with dichloromethane containing 5% methanol removed the complex. In order to purify the complex, this material was recrystallized from a concentrated solution in dichloromethane by adding *n*-pentane. This procedure was repeated until no changes were observed in the UV-visible and IR spectra. The complex with L=4-phenylpyridine was available from a previous work [15].

Elemental analysis: for L=4-(4′-nitrobenzyl)-pyridine calculated C, 45.20; N, 7.90; H, 3.10. Found C, 45.49; N, 7.75; H, 2.94. For L=3-phenylpyridine calculated C, 50.20; N, 4.70; H, 3.10. Found C, 48.95; N, 4.48; H, 2.93. For L=4,4′bipyridine calculated C, 46.00; N, 9.50; H, 2.70. Found C, 45.70; N, 9.72; H, 2.90. For L=4-benzylpyridine calculated C, 51.80; N, 4.50; H, 3.60. Found C, 52.19; N, 4.44; H, 3.80. Spectroquality dichloromethane (Mallinckrodt), ethanol (Mallinckrodt) methanol (Mallinckrodt) and acetonitrile (Mallinckrodt) were dried over molecular sieves.

In Fig. 1 the structural formulae of the ligands are shown.

2.2. Equipment and procedures

The flash photolysis apparatus for the study of reaction kinetics and the measurement of transient absorption or emission spectra in the ns to ms time domain has been described elsewhere [16]. In these experiments, 10 ns flashes of monochromatic light were generated with a Nd:YAG (Quanta Ray) or a N_2 (Laser Photonics, PRA/Mode/UV-24) laser, respectively.

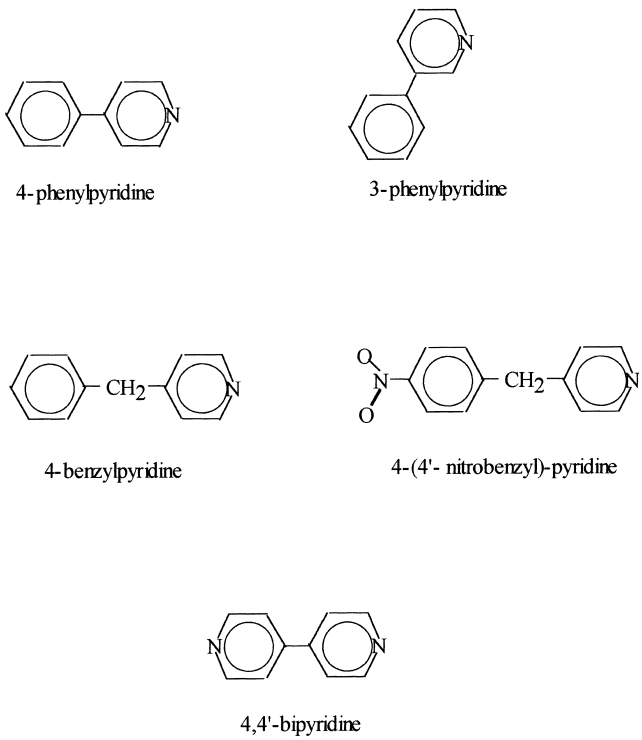

Fig. 1. Structures of the monoazine ligands.

The luminescence of the Re(I) complexes was investigated in an SLM-Aminco-4800 spectrofluorimeter connected to a PC. Spectra were corrected for differences in spectral response and light scattering. Solutions were deaereated with O_2-free nitrogen in a gas-tight apparatus before recording the spectra. Spectra at T=77 K were recorded with samples immersed in liquid nitrogen. Ethanol/methanol mixtures (4:1 v/v) were used as solvents for emission measurements in the glassy state.

UV-visible spectra were recorded on a CARY 3 spectrophotometer and infrared spectra on a Shimadzu IR-435 spectrophotometer.

Cyclic voltammmetry was performed in acetonitrile solutions at a glassy carbon working electrode with 0.1 M tetrabutylammonium hexafluorophosphate as a supporting electrolyte. The rhenium complex concentration was kept at 1×10^{-3} M and the ferrocene/ferricinium couple was used as the standard for all the experiments. For those measurements a LYP M2 potentiostat, a 3-module LYP sweep generator, and a Houston Omnigraphic 2000 pen recorder were used.

3. Results and discussion

3.1. Carbonyl stretching frequency

Infrared spectra were recorded in solid state. In the carbonyl region, a pattern of three peaks typical of fac-$Re(CO)_3L_3^+$ complexes [14] was observed. The highest energy peak was found at 2030±2 cm^{-1}. The two lower energy peaks were poorly resolved and they appeared as broad bands at 1906±4 and 1926±4 cm^{-1}, respectively.

3.2. Redox properties

Half-wave potentials were determined by cyclic voltammetry and are listed in Table 1. The complexes displayed oxidation in the +1.38 to +1.78 V range (vs. SSCE) and one or two reductions between −0.63 to 1.88 V. The oxidation wave was assigned to the metal-centered process, $Re^{2+/+}$, and the first reduction peak to the ligand-centered $L^{0/-}$ process.

3.3. Electronic absorption spectra

Absorption spectra for the complexes were obtained in methylene chloride, and the results are shown in Table 1. The spectra were very similar to those of analogous Re(I) tricarbonyl complexes, [16–18] and the assignments have been made accordingly. A typical spectrum consisted of a strong UV band, assigned as ligand-centered (IL) transitions. A band or a broad shoulder were observed at lower energy in every case, and the lowest energy feature is assigned as an MLCT transition, $d_\pi(Re\ (I))\rightarrow\pi^*(L)$.

Table 1
Redox and UV-visible spectral data for $Re(CO)_3L_3^+$ complexes at room temperature

Ligand	E,V		ΔE,V	λ/nm (ε/M^{-1} cm^{-1})[b]
	Oxidation	Reduction		
4-phenylpyridine	+1.73[a] (100 mV)	−1.61 (irrev)	3.34	281 (52000); 301 (sh)
3-phenylpyridine	+1.44 (irrev)	−1.70 (irrev)	3.14	280 (27000)
4-benzylpyridine	+1.64[a] (75 mV)	−1.88[a] (90 mV)	3.52	285 (41300); 315 (sh)
4-(4′nitrobenzyl)-pyridine	+1.76[a] (175 mV)	−0.63 (irrev)	2.39	267 (21000)
4,4′-bipyridine	+1.38[a](100 mV)	−1.19[a] (10 mV)	2.57	245 (65000); 319 (23600)

(a) Potentials estimated as $1/2(E_p(ox)+E_p(red))$. Scan rate=200 mV s^{-1}. Between brackets, $\Delta E_p=E_p(ox)-E_p(red)$. (b) Data from dichloromethane solutions.

Since the MLCT band mostly occurs as a broad shoulder (in some cases it just means a change in the slope of the band), the exact position of the band and extinction coefficient could not be determined for each case. It is worthy to note that when the ligand is 4,4′-bipyridine the lower energy band is well defined and better separated from those absorptions due to intraligand transitions.

3.4. Transient absorption spectra

In Fig. 2 the transient absorption spectra of the complexes under study can be seen. These spectra can be assigned to the corresponding emitting excited states; the assignment is made on the basis that the absorption lifetimes are the same, within experimental error, to those measured for the luminescence decays. These spectra resemble those of $[Re(CO)_3L_3]$ radicals [14] and both are quite similar to those of $L^{\bullet -}$ radicals [19–21], suggesting structural similarities.

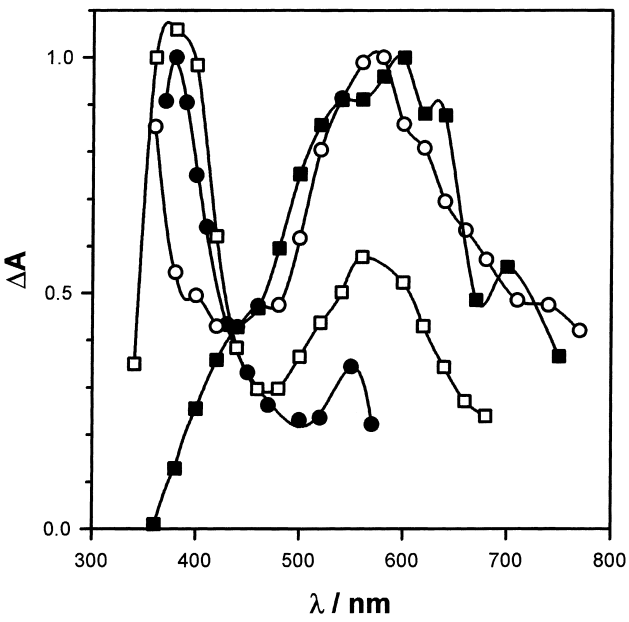

Fig. 2. Transient absorption spectra of the $Re(CO)_3L_3^+$ complexes obtained after 355 nm flash irradiations of dichloromethane solutions at room temperature. (●) 3-phenylpyridine, (□) 4-phenylpyridine, (○) 4,4′-bipyridine, (■)4-benzylpyridine.

3.5. Emission at room temperature

In dichloromethane the complexes displayed broad emission spectra (Fig. 3) which have been assigned as MLCT-based luminescence, typical of this type of complex. [14,16–18]. Nevertheless, a contribution from intra-ligand excited state (^{3}IL or $^3\pi\pi^*$) cannot be discarded (see below). Apart from a high-energy shoulder for the complex with L=4-(4′-nitrobenzyl)pyridine, the spectra were unstructured, with λ_{max} varying from 498 to 615 nm in methylene chloride and from 505 to 635 nm in acetonitrile.

For the complexes the trend in emission energy followed the thermodynamic energy gap (see Fig. 4). As the ease of reducing the ligand increases the energy of the MLCT excited state decreases. However, the complexes with L=4-(4′-nitrobenzyl)-pyridine and 4-benzylpyridine showed an anomalous behavior indicating that in these cases the electrochemical reduction process does not involve the same orbitals as in the photo-induced charge transfer. In the case of the complex with L=4-(4′-nitrobenzyl)-pyridine, a very low reduction peak (L/L^-) (see Table 1) would imply that the nitro group is actually reduced during voltammetry.

Emission maxima were solvent-dependent, which is a characteristic of MLCT emission. In acetonitrile, λ_{max} is red-shifted by 20–32 nm compared to results in methylene chloride and lifetimes were shorter in the more polar solvent. The complexes with L=3-phenylpyridine and 4-phenylpyridine showed much smaller solvent dependence. Emission maxima shifted by only 7 and 8 nm, respectively, but lifetimes were shorter by approximately a factor of 2.

Lifetimes obtained at room temperature by irradiating at 355 nm are summarized in Table 2. Emission lifetimes range from a few ns to 2.5 μs depending on the solvent. In methylene chloride all complexes present biexponential (τ_1 and τ_2 in Table 2) decay but in acetonitrile only the complex with L=3-phenylpyridine keeps this behavior meanwhile the others become monoexponential.

3.6. Emission at low temperature

Emission measurements made at 77 K in frozen glasses showed different behaviors. (see Fig. 3) The spectra of the complexes with L=3-phenylpyridine and 4-benzylpyridine were structured with vibrational spacing similar to that

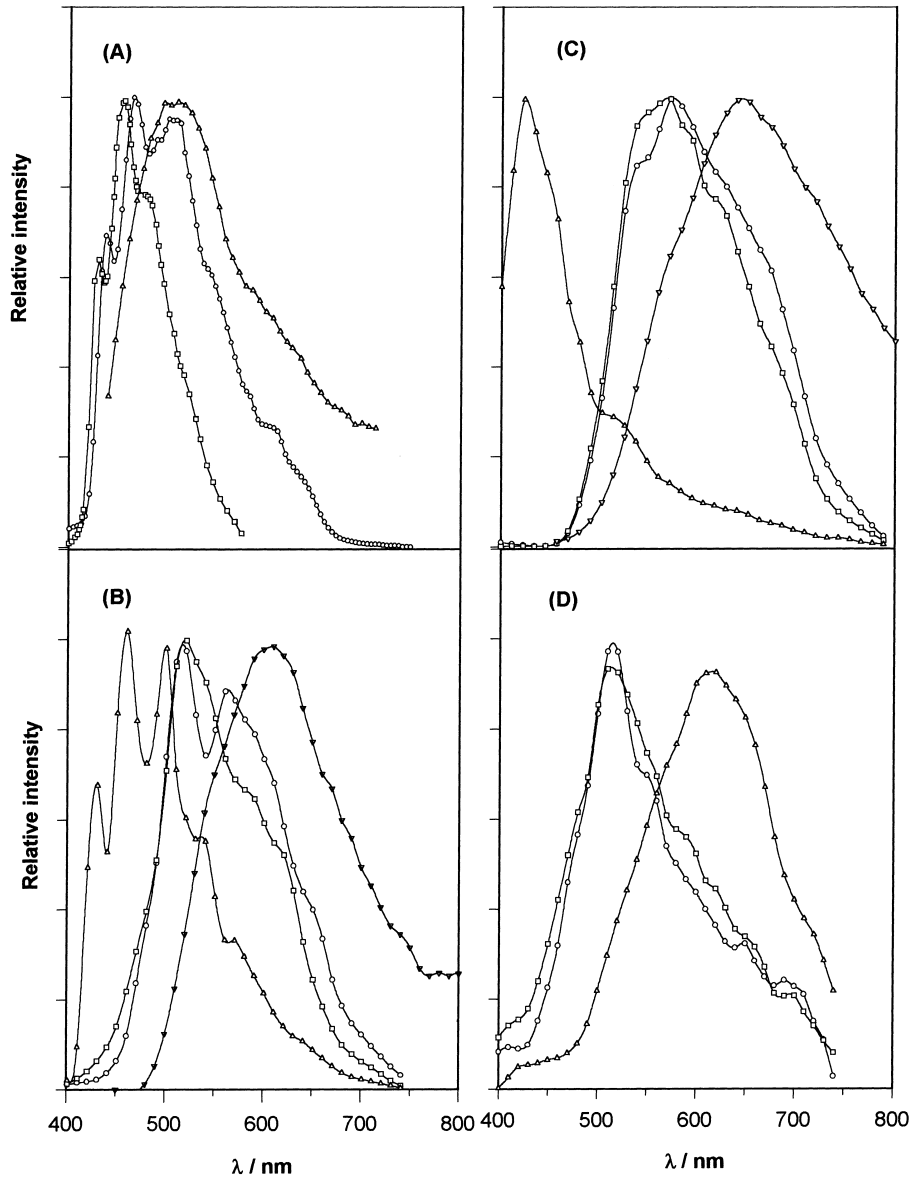

Fig. 3. Emission spectra of the $Re(CO)_3L_3^+$ complexes and the free ligand L in different experimental conditions: (A) $Re(CO)_3$(3-phenylpyridine)$_3^+$: (○) λ_{ex}=350 nm, 77K, (△) λ_{ex}=420 nm, room temperature, 3-phenylpyridine: (□) 77K[a]. (B) $Re(CO)_3$(4-benzylpyridine)$_3^+$: (○) λ_{ex}=370 nm, 77K, (□) λ_{ex}=350 nm, 77 K, (▽)=360 nm, room temperature, 4-benzylpyridine: (△)=370 nm, 77 K. (C) $Re(CO)_3(4,4'$-bipyridine$)_3^+$: (○) λ_{ex}=350 nm, 77 K, (□) λ_{ex}=370 nm, 77 K, (▽) λ_{ex}=400 nm, room temperature, 4,4′-bipyridine: (Δ) λ_{ex}=370 nm, 77 K. (D) $Re(CO)_3$(4-(4′-nitrobenzyl)pyridine$)_3^+$: (○) λ_{ex}=370 nm, 77 K, (△) λ_{ex}=400 nm, room temperature, 4-(4′-nitrobenzyl) pyridine: (□) λ_{ex}=370 nm, 77 K. [a]Taken from [32].

Table 2
Corrected emission maxima and lifetimes of the $Re(CO)_3L_3^+$ complexes taken at room temperature in dichloromethane and acetonitrile

Ligand	CH_2Cl_2			CH_3CN		
	λ_{max}(nm)	τ_1(ns)	τ_2(ns)	λ_{max} (nm)	τ_1(ns)	τ_2(ns)
4-phenylpyridine	498	4180	1250	505	2450	–
3-phenylpyridine	510	1880	220	518	907	36
4-benzylpyridine	603	1214	50	640	291	–
4-(4′nitrobenzyl)-pyridine	598	170	41	630	≈20	–
4,4′-bipyridine	615	1260	93	635	439	–

The excitation wavelength was 355 nm.

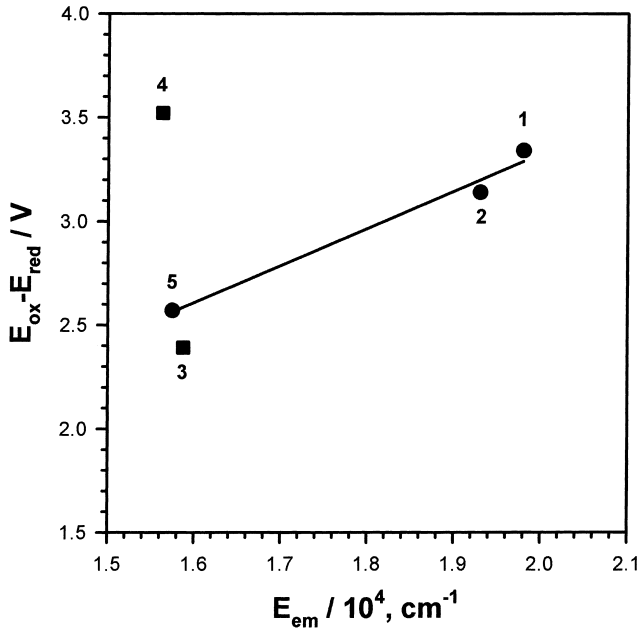

Fig. 4. Correlation between redox potentials and emission energy for the $Re(CO)_3L_3^+$ complexes in acetonitrile solutions: (1) L=4-phenylpyridine, (2) L=3-phenylpyridine, (3) L=4-(4′-nitrobenzyl) pyridine, (4) 4-benzylpyridine and (5) 4,4′-bipyridine. In Fig. 4 the emitting state energy was taken as the energy of the emission maximum, while not actually equal to the state energies, it should track the state energies for a homologous series of complexes.

observed in the free ligand. The emission spectra were dependent on excitation energy showing that emission is due to two emitting excited states. However, the emission spectrum for the complex with L=4,4′-bypiridine presented only some features and that with L=4-(4′-nitrobenzyl)-pyridine was quite like that observed for the free ligand. The emission spectrum of the complex with L=4-phehyl-pyridine has been previously reported [22] showing similar behavior to that observed when L=3-phenylpyridine.

The emission decays in ethanol/methanol glasses, measured irradiating at 337 nm, were biexponential. The values of the observed lifetimes ranged from 14 to 2000 μs (see Table 3). The biexponential behavior and the spectral features observed at low temperature agree with the presence of two emitting excited states.

The changes in emission characteristics can be accounted for in terms of the sensitivity of MLCT state energies to solvent properties and the rates of solvent relaxation relative to emission decay time. The MLCT state sensitivity arises from the significant change in dipole moment that accompanies MLCT excitation. Due to this dipole moment, the MLCT excited state formed initially is non-equilibrated with respect to solvent orientation and internal geometry. It will, however, be vibrationally equilibrated for the current solvent environment, even if this is well above the thermodynamically most stable conformation. At room temperature complex and environment can relax to the thermally equilibrated excited (thexi) state on a time scale that is short compared to the decay time. In the thexi state, the solvent and internal

Table 3
Lifetimes of the $Re(CO)_3L_3^+$ complexes in ethanol/methanol (4:1) at 77 K

Ligand	τ_1 (μs)	τ_2 (μs)
4-phenylpyridine	569	1564
3-phenylpyridine	263	2083
4-(4′-nitrobenzyl) pyridine	14	64
4-benzylpyridine	16	83
4,4′-bipyridine	20	60

Irradiation wavelength was 337 nm.

geometry of the complex are at their lowest energy configuration. Equilibration causes a significant drop in the energy of the initially formed MLCT state. In a rigid glass at 77 K, formation of the thexi state cannot occur during the lifetime of the excited state, and emission will arise from the higher energy unequilibrated form. In contrast, the IL states in our systems do not involve large changes in dipole moment, and the ligand state energies are largely insensitive to solvent and to relaxation processes following excitation.

3.7. Energy gap law

Most azine complexes of Re(I) are sufficiently weak emitters [23,24] that lifetimes are dominated by non-radiative decay. In this limit, the following relationships hold.

$$\tau^{-1} = k_r + k_{nr} \quad (1a)$$

$$\phi_{em} = \tau k_r \quad (1b)$$

$$\tau^{-1} \sim k_{nr} \quad (1c)$$

In Eqs. (1a), (1b) and (1c), k_r and k_{nr} are the rate constants for radiative and non-radiative decay, ϕ_{em} is the emission quantum yield, and τ is the lifetime. The biexponential behavior can be rationalized assuming parallel relaxations of two excited states, for example, ^{3}MLCT and ^{3}IL, with intrinsic rates and the shorter lifetime can be attributed to the ^{3}MLCT state. There are very large variations in MLCT excited-state lifetimes with variations in the pyridinic ligand (see Table 3). Radiationless decay rates depend on the energies of the emitting states; the lower the energy of an emitting state, the more strongly it couples with the ground state and the larger k_{nr}. In Fig. 5 ln k_{nr} (k_{nr} was calculated from τ values obtained in dichloromethane) is plotted against the zero–zero energy difference showing poor agreement with the energy gap law.

In the low-temperature ($\hbar\omega_M >> kT$)weak-vibrational-coupling ($(E_{em}(0-0)/\hbar\omega_M S_M) \gg 1$) limit, the energy gap law can be written as:

$$\ln k_{nr} = \ln\beta_o - S_M - \frac{\gamma_o E_{em}(0-0)}{\hbar\omega_M} + (\chi_o/\hbar\omega_M)(kT/\hbar\omega_M)(\gamma_o+1)^2 \quad (2)$$

$$\beta_o = (C^2\omega_k)(\pi/(2\hbar\omega_M(E_{em}(0-0) - \hbar\omega_k)))^{1/2} \quad (3)$$

χ_o is four times the classical solvent vibrational trapping or re-organizational energy associated with the transfer of the

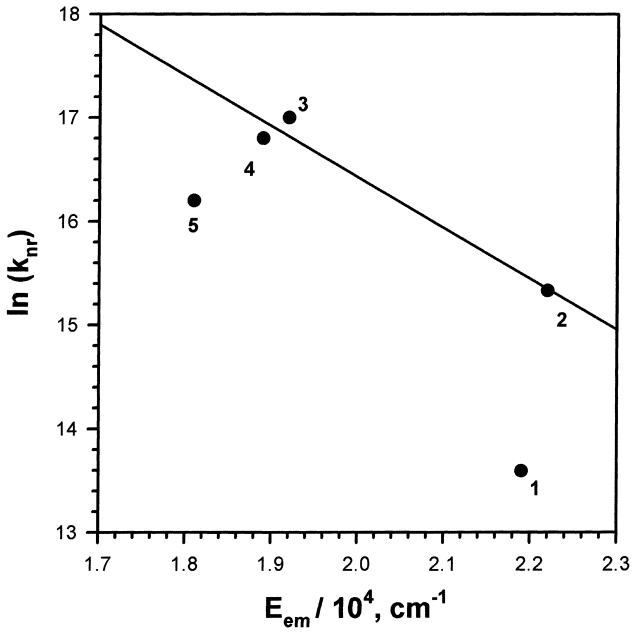

Fig. 5. Plot of ln (k_{nr}) vs. E_{00} at room temperature in dichloromethane for $Re(CO)_3L_3^+$ complexes: (1) 4-phenylpyridine, (2) 3-phenylpyridine, (3) 4-(4′-nitrobenzyl) pyridine, (4) 4-benzylpyridine, (5) 4,4′-bipyridine. The E_{00} values were obtained according to Eqs. (6) and (7). For the 4-(4′-nitrobenzyl) pyridine complex, where no good fitting was obtained, E_{00} was estimated from the spectrum in Fig. 3. Not much difference, for the others complexes, was observed between the values obtained from this procedure and that coming from the spectral fitting.

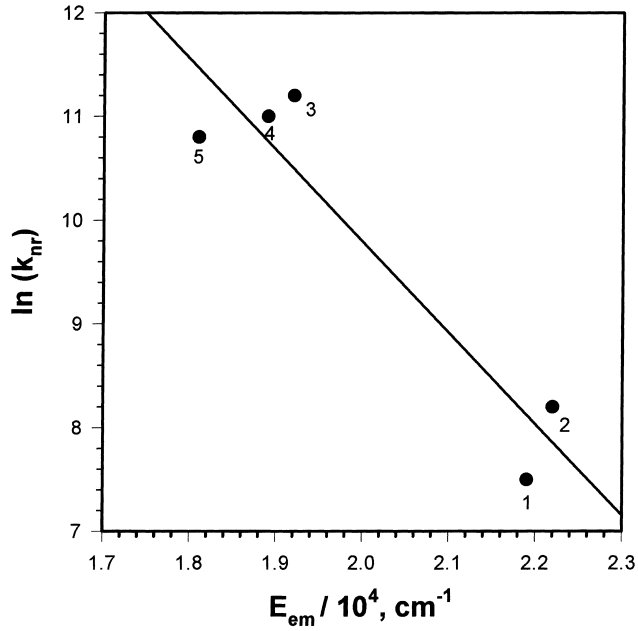

Fig. 6. Plot of ln (k_{nr}), at 77 K, vs. E_{00} in dichloromethane for $Re(CO)_3L_3^+$ complexes: (1) 4-phenylpyridine, (2) 3-phenylpyridine, (3) 4-(4′-nitrobenzyl) pyridine, (4) 4-benzylpyridine, (5) 4,4′-bipyridine. To use those RT E_{00} values for 77 K experiments implies assuming that the loss of MLCT excited state stabilization energy is the same for all the complexes. Actually, it depends on the magnitude of the dipole moment gap between the ground and the excited state and on the matrix glass. However, we believe that this assumption does not invalidate the interpretation of the results.

electron from the ligand to the metal. ω_M ($=2\pi\nu_M$) is the angular frequency of the acceptor vibration or vibrations. ω_k ($=2\pi\nu_k$) is the angular frequency of the promoting vibration and C^2 the corresponding nuclear momentum matrix element. $S_M(=1/2\Delta_M^2)$ is a measure of the extent of excited-state distortion in the acceptor vibration. Δ_M^2 is the dimensionless fractional displacement in the acceptor vibration between equilibrium geometries of the ground and excited states. In terms of a displacement coordinate Q (in cm), the dimensionless mass- and frequency-weighted coordinate q is given by $q = Q(M\omega/\hbar)^{1/2}$ where M is reduced mass of the vibration. The shift in the equilibrium position of the ground state relative to the excited state for the mth normal vibration is given by $\Delta M = q_c^e - q_c^g$, where q_c^e and q_c^g are the equilibrium normal coordinates for the excited and ground states. $E_{em}(0–0)$ is the emission energy for the $\nu'_M = 0 \rightarrow \nu_M = 0$ vibrational component. And γ_o is defined as

$$\gamma_o = \ln\frac{E_{em}(0-0) - \hbar\omega_k}{\hbar\omega_M S_M} - 1 \approx \ln\frac{E_{em}(0-0)}{\hbar\omega_M S_M} - 1 \qquad (4)$$

Since the term linear in E_{00} is the most important one in Eq. (2), the approximation in Eq. (5) is typically found to hold [1].

$$\ln k_{nr} \propto 2\pi\gamma_0 E_{00}/h\omega_M \qquad (5)$$

The acceptor ligand appears in this relationship in two ways. One is the energy gap. The other is the extent of excited-state distortion as measured by Δ_M. Fig. 5 shows that the energy gap law is badly followed at room temperature (i.e. complexes with L=4-phenylpyridine and L=3-phenylpyridine present very closed E_{00} values though their respective k_{nr} values differ by almost two orders of magnitude). However, from data at 77 K, the plot of ln k_{nr} versus E_{em} (see Fig. 6) shows a slightly better agreement with the simplified energy gap law. To obtain more clues to rationalize these facts the excited state distortion is analyzed next.

3.8. Emission spectral fitting

The procedure for the Franck–Condon analysis of emission spectral profiles has been described in detail elsewhere [25]. Only a brief outline of the two-mode analysis is presented here.

Calculated emission profiles were generated by using

$$I(\nu) = \sum_{\nu_M}^{\infty}\sum_{\nu_L}^{\infty}[(\nu_{00} - \nu_M\nu_M - \nu_L\nu_L)/\nu_{00}]^4 \times [(S_M^{V_M})/\nu_M!] \times [(S_L^{V_L})/\nu_L!] \times \exp\{-4(\ln 2)[(\nu - \nu_{00} + \nu_M\nu_M + \nu_L\nu_L)/\Delta\nu_{1/2}]^2\} \qquad (6)$$

$$I_{em}(\nu)/I_{em}(\nu_{max}) = N \times I(\nu) \qquad (7)$$

where $I_{em}(\nu)$ and I_{em} (ν_{max}) represent the observed emission intensity at frequency ν (in cm^{-1}) and the emission intensity

at ν_{max} (the frequency of the emission maximum), respectively. In Eq. (6), v_M and v_L are the vibrational quantum numbers for high (ν_M) and low frequency (ν_L) vibrational progressions of the acceptor modes. In the band shape equation $I(\nu)$ is the intensity of the $v_M^* = 0$, $v_L^* = 0$ to v_M=n_M, v_L=n_L transition relative to the intensity of the $v_M^* = 0$, $v_L^* = 0$ to v_M=0, v_L=0 transition, the so-called 0–0 transition, ν_{00}. The summation was carried out over six levels of vibrations ν_M and ν_L (v_M=0→5 and v_L=0→5). S_M and S_L are the electron vibrational coupling constants for the high and low frequency modes, respectively, and $\Delta\nu_{1/2}$ is the full width at half-maximum of the 0–0 vibrational component of the emission. N is a constant introduced in the fitting equation due to the shift between ν_{max} and ν_{00}. In the fitting procedure, ν_M was fixed at 1420 cm^{-1}, and the remaining six parameters, namely, ν_{00}, ν_L, S_M, S_L, $\Delta\nu_{1/2}$ and N, were varied to obtain the best match between the calculated and experimental spectral profiles. For purposes of spectral fitting the emission spectra were converted from having abscissa linear in wavelength, which is characteristic of the emission spectrometer used, to an abscissa linear in energy by the method described in the literature [25]. Results of these analyses are given in Table 4 while a representative example of such a fit is illustrated in Fig. 7. The frequencies obtained from the spectral fitting should be interpreted as a weighted average of all modes that contribute to the excited state decay. The ca. 1420 cm^{-1} frequency needed to fit our data therefore suggests a dominance of in-plane carbon–carbon skeletal vibration [26]. On the other hand, though no distinct progression due to the low frequency modes related to the ligand–metal bond vibration appears in the spectra, the quality of the spectral fits relies on their inclusion.

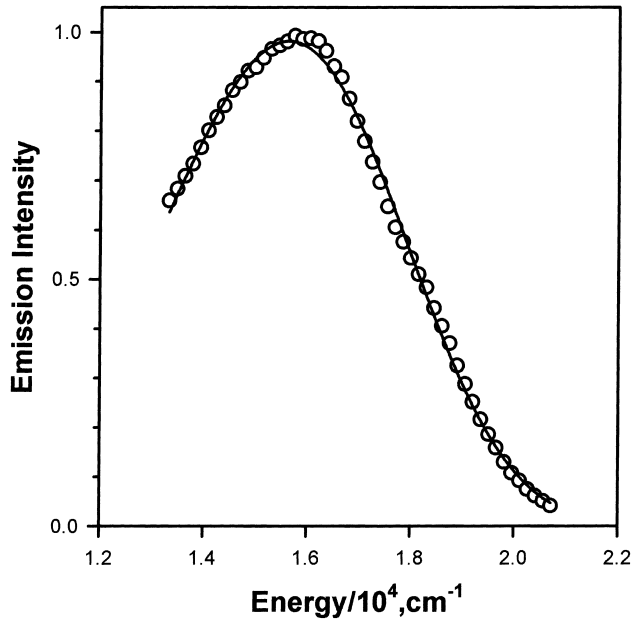

Fig. 7. Spectral analysis of the room temperature emission spectrum of $Re(CO)_3$ $(4,4'\text{-bipyridine})_3^+$. The open circles represent the experimental emission data and the full line the calculated fits.

3.9. Excited state delocalization

The important parameter from the emission spectra fits, as pertains to the present discussion, is the value of S_M. It can be seen from Table 4 that there is a drop of this value from 3.51, for the complex with L=3-phenylpyridine, to 2.43, when L=4,4′-bipyridine. The last one agrees very well with that previously obtained [15] for the complex with L=4-phenylpyridine (S_M=2.42).

From experimental observations and theoretical calculations [27–29], it has been proposed that, for 4,4′-bipyridine, and 4-phenylpyridine ligands of the ground-state geometry the lowest energy conformation is one in which there is a 45° twist angle between the two ring systems [29]. However, for the corresponding radicals, $L^{\bullet -}$, the lowest energy conformation is one in which the reduced species achieves a coplanar delocalized structure. Similarly, in the MLCT excited state the electron should be delocalized over both rings of the acceptor ligand [30,31] attenuating the effect of antibonding orbital population by distributing electron density over a larger number of bonds. The net result would be a decrease in Δ_M along all coordinates sensitive to electron density in the π^* orbital. This delocalization is not possible for 4-benzylpyridine and 4-(4′-nitrobenzyl)-pyridine due to the fact that the connection between the two rings is made through the methylene group. For 3-phenylpyridine the quinoid structure cannot be drawn [32] and, moreover, the extent of intraligand delocalization is altered because the rotation of the phenyl group in position 3 is hindered by the other 3-phenylpyridine ligands bonded to the metal. As a consequence, k_{nr} for the complexes with L=4-benzylpyridine, 4-(4′-nitrobenzyl)-pyridine and 3-phenylpyridine increases relative to the complex with L=4-phenylpyridine and 4,4′-bipyridine making results in Fig. 5 rational.

Due to the ligand conformational change that exists between the ground and excited states for L=4-phenylpyridine and 4,4′-bipyridine their photophysical properties should be highly dependent upon solvent viscosity; therefore, in going from fluid solution to frozen media intraligand rotation becomes difficult and electronic delocalization

Table 4
Emission spectral fitting parameters for $Re(CO)_3L_3^+$ (L=3-phenylpyridine and 4,4′-bipyridine) from dichloromethane solutions at room temperature

Ligand	E_{00}, cm^{-1}	ν_M, cm^{-1}	ν_L cm^{-1}	S_M	S_L	$\Delta\nu_{1/2}$, cm^{-1}	N
3-phenylpyridine	22 550	1420	427	3.51	0.51	2402	0.10
4,4′ bipyridine	17 834	1420	427	2.43	0.63	3670	0.15

would be altered. At 77 K the higher k_{nr} values for the complexes with L=4-phenylpyridine and 4,4′-bipyridine (Fig. 6) could be attributed to the loss of stabilization due to electron delocalization in the excited state.

Acknowledgements

This work was supported in part by the Consejo Nacional de Investigaciones Científicas y Técnicas (CONICET) de la República Argentina, Comisión de Investigaciones Científicas de la Provincia de Buenos Aires (CICBA) and Fundación Antorchas. E.W wishes to thank CONICET for a research graduateship. M.R.F thanks Dr. G. Ferraudi for hosting his visit to Notre Dame Radiation Laboratory and to the Fulbright Commission for a scholarship. Emission spectra were taken at INIBIOLP. We thank Dr. H. Garda for hosting our visits to INIBIOLP.

References

[1] E.M. Kober, J.C. Marshall, W.J. Dressick, B.P. Sullivan, J.V. Caspar, T.J. Meyer, Inorg. Chem. 24 (1985) 2755–2763.
[2] G.H. Allen, R.P. White, D.P. Rillema, T.J. Meyer, J. Am. Chem. Soc. 106 (1984) 2613–2620.
[3] E.M. Kober, J.V. Caspar, R.S. Lumpkin, T.J. Meyer, J. Phys. Chem. 90 (1986) 3722–3734.
[4] R.M. Leaslure, L.A. Sacksteader, D. Nesselrodt, G.A. Reitz, J.N. Demas, B.A. Degfroff, Inorg. Chem. 30 (1991) 1930–1939.
[5] J.V. Caspar, T.J. Meyer, J. Phys. Chem. 87 (1983) 952–957.
[6] R.S. Lumpkin, T.J. Meyer, J. Phys. Chem. 90 (1986) 5307–5312.
[7] L. Sacksteader, A.P. Zipp, E.A. Brown, J. Sttreich, J.N. Demas, B.A. De Graff, Inorg. Chem. 29 (1990) 4335–4340.
[8] V. Balzani, F. Scandola, Supramolecular Photochemistry, Ellis Horwood, Chichester, UK, 1991.
[9] M.A. Fox, M. Chanon, (Eds.), Photoinduced Electron Transfer, Elsevier, New York, 1988.
[10] G.J. Ferraudi, Elements of Inorganic Photochemistry, Wiley, New York, 1988.
[11] M. Bixon, J. Jortner, J. Chem. Phys. 48 (1968) 715.
[12] F.R. Freed, J. Jortner, J. Chem. Phys. 52 (1970) 6272.
[13] R. Englman, J. Jortner, J. Mol. Phys. 18 (1970) 145.
[14] G. Ruiz, E. Wolcan, M.R. Féliz, J. Photochem. Photobiol. A: Chem. 101 (1996) 119–125.
[15] G. Ruiz, F. Rodriguez-Nieto, E. Wolcan, M.R. Féliz, J. Photochem. Photobiol. A: Chem. 107 (1997) 47–54.
[16] M.R. Feliz, G. Ferraudi, H. Altmiller, J. Phys. Chem. 96 (1992) 258–264.
[17] P.J. Giordano, M.S. Wrighton, J. Am. Chem. Soc. 101 (1979) 2888–2891.
[18] P.J. Giordano, S.M. Fredericks, M.S. Wrighton, D.L. Morse, J. Am. Chem. Soc. 100 (1978) 2257–2259.
[19] G. Buntinx, P. Valat, V. Wintgens, O. Poizat, J. Phys. Chem. 95 (1991) 9347–9352.
[20] O. Poizat, G. Buntinx, P. Valat, V. Wintgens, M. Bridoux, J. Phys. Chem. 97 (1993) 5905–5910.
[21] G. Buntinx, R. Nasbrecki, O. Poizat, J. Phys. Chem. 100 (1996) 19380–19388.
[22] G. Ferraudi, M.R. Féliz, E. Wolcan, I. Hsu, S.A. Moya, J. Guerrero, J. Phys. Chem. 99 (1995) 4929–4934.
[23] A.P. Zipp, L. Sacksteder, J. Streich, A. Cook, J.N. Demas, B.A. De Graff, Inorg. Chem. 32 (1993) 5629–5632.
[24] K.S. Schanze, D.B. MacQueen, T.A. Perkins, L. Cabana, A. Coord. Chem. Rev. 122 (1993) 63–89.
[25] J.V. Caspar, T.D. Westmoreland, G.H. Allen, P.G. Bradley, T.J. Meyer, W.H. Woodruff, J. Am. Chem. Soc. 106 (1984) 3492–3500.
[26] D. Burget, P. Jacques, E. Vauthey, P. Suppan, E. Haselbach, J. Am. Chem. Soc., Faraday Trans. 90(17) (1994) 2481.
[27] W.D. Bates, P. Chen, C.A. Bignozzi, J.R. Shoonover, T.J. Meyer, Inorg. Chem. 34 (1995) 6215–6217.
[28] L. Ould-Moussa, O. Poizat, M. Castellá-Ventura, G. Buntinx, E. Kassab, J. Phys. Chem. 100 (1996) 2072–2082.
[29] N.H. Damraver, T.R. Boussie, M. Devenney, J.K. McCusker, J. Am. Chem. Soc. 119 (1997) 8253–8268.
[30] C. Turro, Y.Y. Chung, N. Leventis, M.E. Kuchenmeister, P.J. Wagner, G.E. Leroi, Inorg. Chem. 35 (1996) 5104–5106.
[31] G.A. Neyhart, C.J. Timpson, W.D. Bates, T.J. Meyer, J. Am. Chem. Soc. 118 (1996) 3730–3737.
[32] J. Kubin, A.C. Testa, J. Photochem. Photobiol. A: Chem. 83 (1994) 91–96.